

Stereoselectivity in intramolecular Diels-Alder reactions of 2,4-pentadienyl butadienamides in the “Remote Stereocontrol Group” approach

A. Z. Patleeva*, D. D. Enchev, G. D. Neykov

Department of Organic Chemistry and Technology, Faculty of Natural Sciences, University of Shumen, Shumen, Bulgaria

Received May 12, 2014; Revised May 26, 2014

Dedicated to Acad. Dimiter Ivanov on the occasion of his 120th birth anniversary

The possible reaction paths of intramolecular pericyclic reactions of buta-2,3-dienoic penta-2,4-dienylamide ([1,5]-sigmatropic shift and subsequent Intramolecular [4+2] cycloaddition, Alder-ene reaction and Intramolecular [4+2] cycloaddition) were modeled as asynchronous concerted processes at semi-empirical, ab initio and DFT theoretical level. The endo/exo and π -diastereofacial stereoselectivity of the amide-tethered IMDA reaction of 2,4-pentadienyl butadienamides was investigated using the “Remote Stereocontrol Group” (RSG) approach. The localized transition states (TS) of the investigated reactions were fully optimized at MP2/6-31G(d) and DFT B3LYP/6-31G(d) levels. The relative TS free energies were calculated to determine the stereochemical outcome of the kinetically controlled reactions.

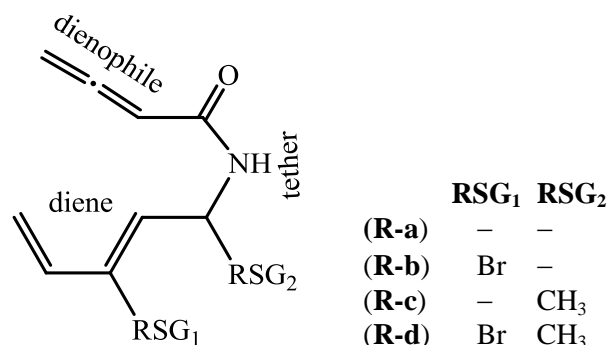
Key words: stereoselectivity, Diels-Alder reaction, Remote Stereocontrol Group, ab initio, DFT, pentadienyl butadienamides

INTRODUCTION

The intramolecular Diels-Alder (IMDA) reaction, popular in organic synthesis for producing polycyclic structures, draws the attention of many theoretical chemists. The computational investigation of IMDA reactions enables predicting chemo-, regio- and stereoselectivities and gives opportunity to examine ways to alter the expected structures, varying conformational, steric and electronic effects independently. It has been established that the stereoselectivity of IMDA reactions could be changed by a suitable choice of diene, dienophile and the type of the tether [1,2]. A large amount of experimental and theoretical studies have investigated the origin of chemical stereoselectivity in intramolecular cycloadditions – reactions of 1,3,8-nonatrienes, 1,3,9-decatrienes and 1,3,10-undecatrienes [3], substituted 3,5-hexadienyl acrylates and acrylamides [4], pentadienyl acrylates [5,6], diene and dienophile linked by a $-(CH_2)_n-$ chain, ($n=1, 2, 3$ и 4) [7]. Despite the existence of computational models of *allene* as *dienophile* in the *intermolecular* Diels-Alder reaction [8,9], models of *intramolecular* cycloadditions are not available.

In this respect we have been interested in modeling the transition structures (TS), predicting and

varying, using *Remote Stereocontrol Group* (RSG), the stereochemical outcome of the IMDA reactions of pentadienyl butadienamides (**R-a**), (**R-b**), (**R-c**) and (**R-d**).



COMPUTATIONAL PROCEDURE

Geometries of the reactants, transition structures (TS) and products were fully optimized at B3LYP/6-31G(d) and MP2/6-31G(d) level. The precursors and the expected products were connected via transition structures using the IRC procedure, Gonzalez-Schlegel method. All structures were characterized as minima (no imaginary frequencies) or a saddle point (1 imaginary frequency) on the potential energy surface (PES) by frequency calculations at the same computational

* To whom all correspondence should be sent:

E-mail: a.patleeva@shu-bg.net

© 2014 Bulgarian Academy of Sciences, Union of Chemists in Bulgaria

level. The calculated total energies, enthalpies and free energies were corrected by zero-point energy (unscaled), estimated from the harmonic frequency calculations under atmospheric pressure and temperature 373K, which we believe is typical for modeled reactions. The relative free energies of the TS at the 373K were calculated to determine the stereochemical outcome of the kinetically controlled reactions.

All calculations were performed using the Firefly QC package [10], which is partially based on the GAMESS (US) [11] source code.

RESULTS AND DISCUSSION

The calculations of the three reaction pathways of the competing intramolecular pericyclic reactions (Fig. 1) were performed at the semi-empirical (AM1, PM3) theoretical level. The aim of the preliminary computations was to evaluate the activation and reaction energies, to determine whether the reactions are feasible, which is particularly important in the absence of experimental data and to compare the competing

processes. Reasonable pericyclic reactions (*reaction path 1* - Intramolecular [4+2] cycloaddition, *reaction path 2* - [1,5]-sigmatropic shift and subsequent Intramolecular [4+2] cycloaddition, *reaction path 3* - Alder-ene reaction) of (**R-a**, **b**, **c**, **d**) were modeled as *asynchronous concerted* processes. The *reaction path 3* (Alder-ene reaction, Fig. 1) was definitely eliminated. Nevertheless, to obtain accurate energies and hence the correct prediction of the preferred cycloadducts, higher levels of theory were required. An adequate geometry for the asynchronous TS, reactants and products was furnished by calculations at the semi-empirical level.

To perform higher level calculations, we used the hybrid B3LYP functional with the 6-31G(d) basis set which has been proven to be particularly successful for modeling TS and energetics of pericyclic reactions [12-14], and the many-body perturbation method of Møller and Plesset (MP2) with the same basis, for estimating the effect of dynamic electron correlation. Despite of the limitations of DFT methods leading to overestima-

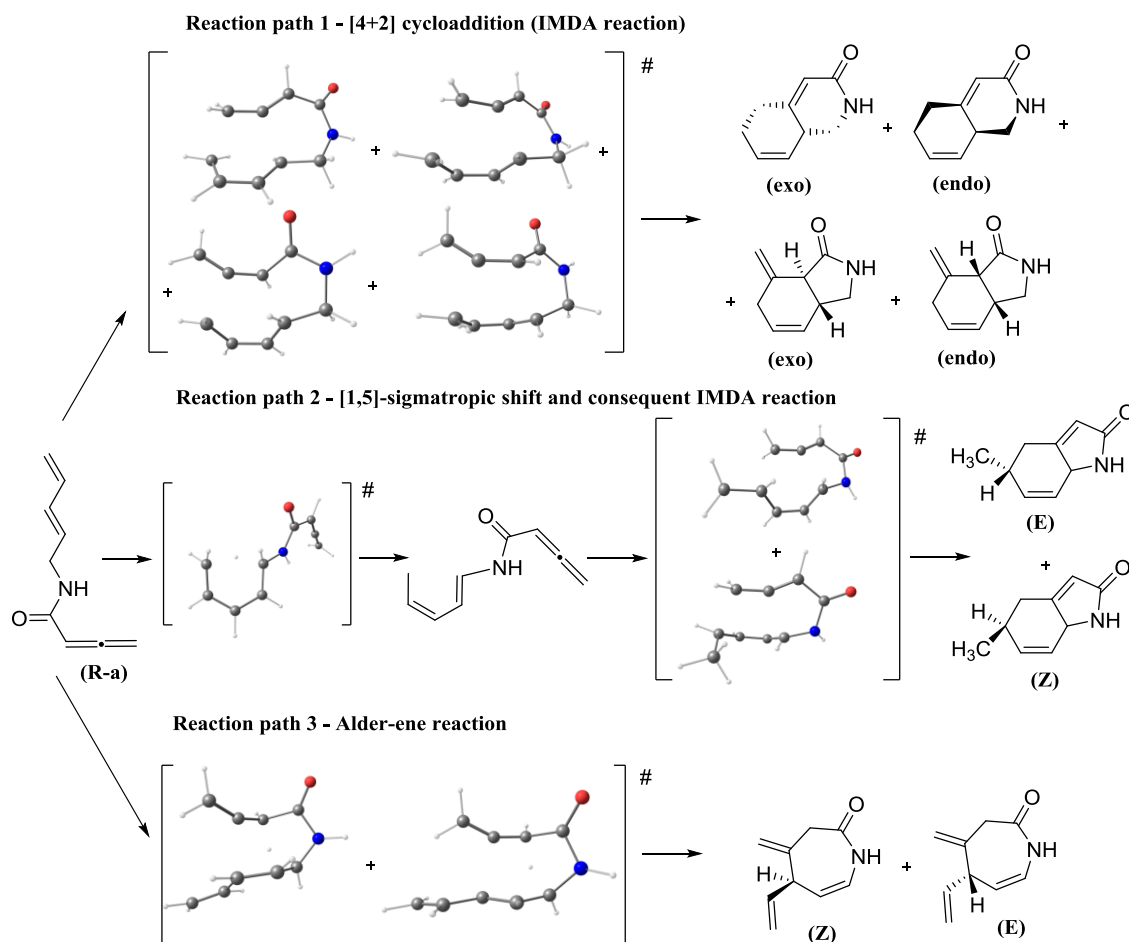


Fig. 1. Modeled pericyclic reactions of buta-2,3-dienoic penta-2,4-dienylamide (**R-a**) at AM1 (presented TS models) semi-empirical computational level.

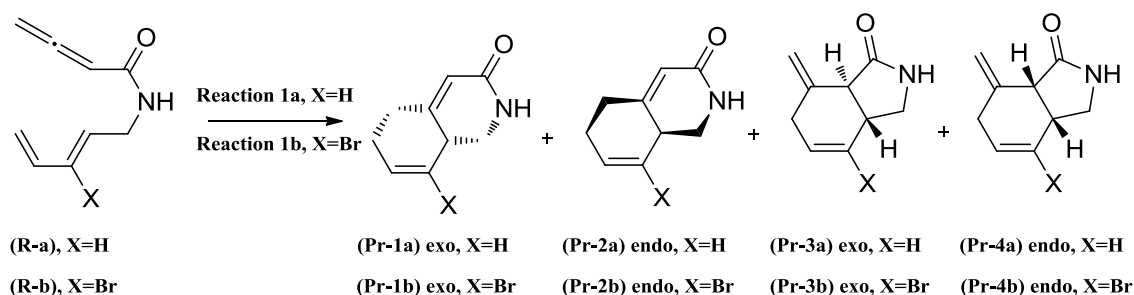


Fig. 2. Modeled IMDA reactions of precursors (R-a) and (R-b); Reactions 1a and 1b.

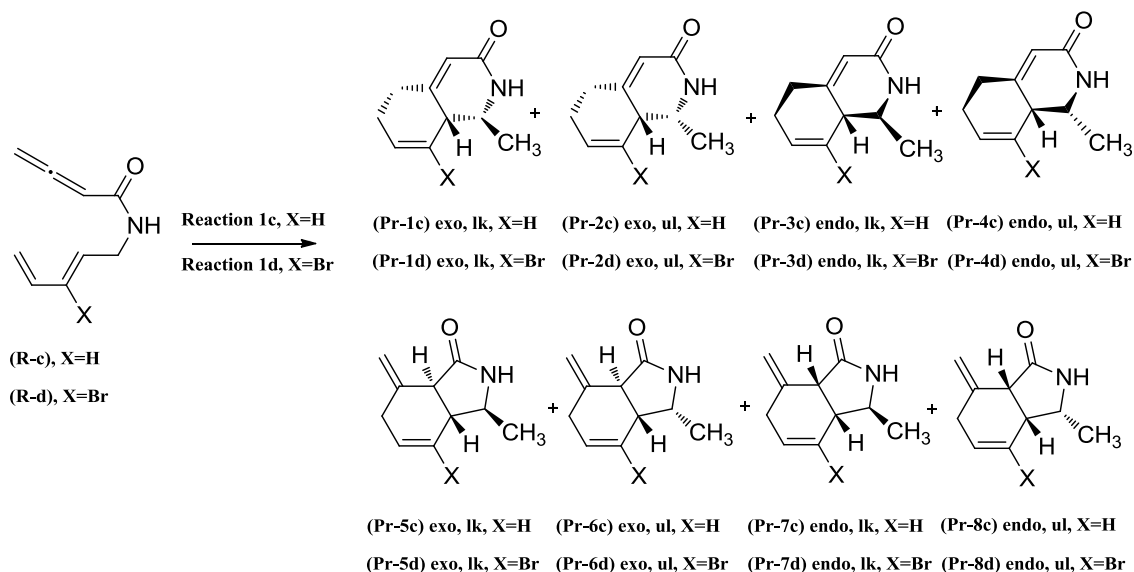


Fig. 3. Modeled IMDA reactions of precursors (R-c) and (R-d); Reactions 1c and 1d.

tion of the energy of conversion of π bonds into σ bonds, which might result in errors in DFT energetics of electrocyclic reactions [15], the functional B3LYP remains very popular due to the balance between accuracy and efficiency.

The Diels-Alder reaction goes primarily in an *endo* rather than an *exo* direction when the product formation is kinetically controlled. It is known that C3 substituent manipulates the stereochemical outcome of IMDA reaction and shifts product distribution toward trans-fused (*exo*) bicyclic products [1], so we have used *bromine*, reported as a successful *RSG* and the *5-methyl tether substituent* - another stereo controlling element which also effectively accelerates the rate of IMDA reactions [3].

Competing IMDA reactions (*reaction paths 1a, 1b, 1c, 1d*) and corresponding [1,5]-sigmatropic shifts (*reaction paths 2a, 2b, 2c, 2d*) are presented on Fig. 2, Fig. 3 and Fig. 4. Computed relative free energies for the competing IMDA Reactions and

corresponding [1,5]-sigmatropic shifts at DFT and ab initio MP2 level are given in Table 1.

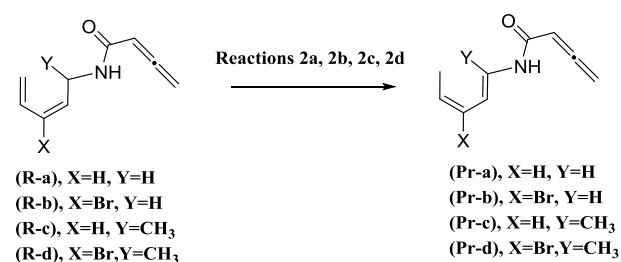


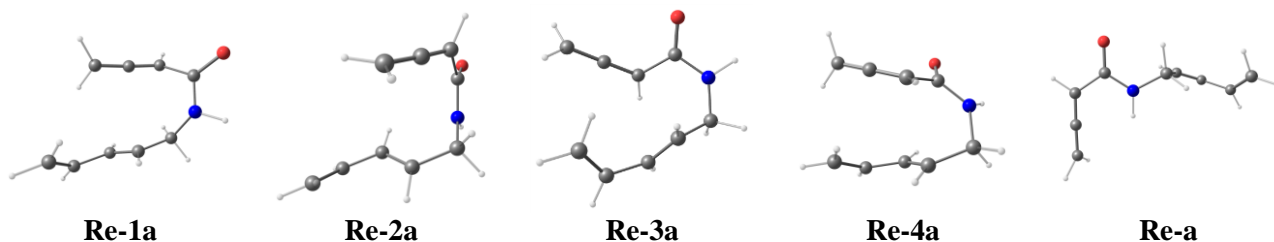
Fig. 4. Modeled [1,5]-sigmatropic shifts of precursors (R-a, R-b, R-c, R-d), Reactions 2a, 2b, 2c, 2d.

The reagents (R-a, b, c, d) are presented by the conformation having the lowest energy. The relative free energy of the proper conformer (Re-n, Fig.5) is the "cost" of reaching suitable configuration for the corresponding transition state and could reach 10-12 kcal.mol⁻¹ (Table 1).

Table 1. Computed free energies (ΔG^\ddagger and ΔG , kcal.mol⁻¹) at 373 K for the competing IMDA Reactions **1a-d** (Fig. 2, Fig. 3) and corresponding [1,5]-sigmatropic shifts (Reactions **2a-d**, Fig. 4) at DFT and ab initio MP2 level.

		$\Delta G^\ddagger/\Delta G$, kcal.mol ⁻¹							
		B3LYP/6-31G(d)				MP2/6-31G(d)			
		a (X=H)	b (X=Br)	c (X=H)	d (X=Br)	a (X=H)	b (X=Br)	c (X=H)	d (X=Br)
Reaction 1	R*	0.00	0.00	0.00	0.00	0.00	0.00	0.00	0.00
	Re-1	11.32	12.38	5.02	4.79	4.44	10.82	7.03	1.97
	Re-2	7.87	9.19	8.95	8.13	4.25	7.43	10.50	7.54
	Re-3	7.39	8.76	9.94	9.24	2.69	10.70	11.66	8.63
	Re-4	7.84	10.73	3.44	6.35	2.52	7.19	4.79	7.09
	(TS-1)	34.53	33.98	28.99	30.08	23.53	25.64	25.36	22.71
	(TS-2)	35.31	35.79	30.87	35.19	23.31	26.19	26.91	27.95
	(TS-3)	39.11	37.73	30.73	32.32	26.07	27.49	26.04	25.86
	(TS-4)	39.83	39.88	29.77	32.57	26.77	27.61	24.90	24.02
	Pr-1	-34.53	-35.08	-39.79	-35.53	-48.44	-42.61	-48.84	-47.73
	Pr-2	-33.18	-31.16	-38.81	-37.87	-51.37	-44.08	-48.69	-50.81
	Pr-3	-26.66	-26.48	-38.29	-37.45	-45.25	-36.63	-45.72	-47.18
Pr-4	-28.46	-27.58	-37.66	-31.11	-47.25	-42.43	-45.22	-44.25	
Reaction 2	a (X=H)	5.27	2.93	0.48	2.33	0.88	3.23	5.54	2.98
	(TS)	31.94	32.19	32.94	34.46	27.10	31.38	34.05	32.91
	Pr	-4.06	-6.24	-5.61	-7.77	-7.46	-4.04	-1.60	-2.19

* The reagents, TS and products are marked as “**Re-n**, **Pr-n**, **TS-n**, **exo/endo**, **lk/ul**”, where lk/ul – Seebach-Prelog descriptors, **n** – the number of the relevant product (Fig. 3). The substrates, TS and cycloadducts of the reactions **1c** and **1d** having high activation energy and hence negligible product distribution are omitted.

**Fig. 5.** The models of the conformations (**Re-1a**, **Re-2a**, **Re-3a** and **Re-4a**, **Re-a**) of the reagent (**R-a**) computed at MP2 level for reactions **1a** and **2a**.

Geometries of the TS having lowest value of ΔG^\ddagger_{rel} for the IMDA reactions **1a**, **1b** and corresponding competing [1,5]-sigmatropic shift, reactions **2a**, **2b** (**TS-a**, **TS-b**) are shown in Fig. 6.

Models of the TS for reactions **1c** and **1d** are shown in Fig. 7. All computed TS are asynchronous with a longer developing peripheral bond (r_1 , Å) then the developing internal bond (r_2 , Å). Calculated differences between r_1 and r_2 (Δr) were used as a measure of asynchronicity (Table 3).

The *exo*-TS are less asynchronous and closer to the TS in Intermolecular Diels-Alder reaction of propadiene and 1,3-butadiene [8]. MP2 calculations significantly increased reaction asynchronicity. The computed forming and breaking bond lengths of the TS are reasonable for pericyclic reactions [13].

The free energy profile of all reactions **1a-1d**, **2a-2d** (Table 1, Fig. 8-reaction **1a**) estimated with MP2 level disfavored reactions **2a-d** – sigmatropic shift. The comparison of the relative free energy of the computed MP2 TS predicted as preferable (**Pr-2a**, no RSG) and (**Pr-4c**, 5-methyl RSG) (*endo*) cycloadducts. Bromine as RSG shifted distribution toward *trans*-fused (*exo*) products (**Pr-1b**, **Pr-1d**) (Table 1, Table 2). In fact, the MP2 calculations determined reaction **1a** as stereo unselective, reaction **1b** – as a reaction with moderate stereoselectivity in favor of the (*exo*) product, reaction **1c** – as a reaction with moderate stereoselectivity toward *cis*-fused (*endo*) product. Using two RSG – bromine and methyl substituents led to increasing amount of (*exo*) products considerably – (**Pr-1d**, *exo*, lk; **Pr-5d**, *exo*, lk).

Table 2. Computed free energies (ΔG^\ddagger and ΔG , kcal.mol⁻¹) at 373 K for the competing IMDA Reactions **1a-d** (Fig. 2, Fig. 3) and corresponding [1,5]-sigmatropic shifts (Reactions **2a-d**, Fig. 4) at DFT and ab initio MP2 level.

		ΔG^\ddagger_{rel} , kcal.mol ⁻¹			
		B3LYP/6-31G(d)		MP2/6-31G(d)	
		a (X=H)	b (X=Br)	a (X=H)	b (X=Br)
Reaction 2	(TS)	0.0	0.0	0.2	5.7
Reaction 1	(TS-1) exo	2.6	1.8	0.0	0.0
	(TS-2) endo	3.4	3.6	2.8	0.6
	(TS-3) exo	7.2	5.5	3.5	1.9
	(TS-4) endo	7.9	7.7	3.8	2.0
		c (X=H)	d (X=Br)	c (X=H)	d (X=Br)
Reaction 2	(TS)	3.9	4.4	9.1	10.2
Reaction 1	(TS-1) exo, lk	0.0	0.0	0.5	0.0
	(TS-2) exo, ul	1.9	5.1	2.0	5.2
	(TS-3) endo, lk	1.7	2.2	1.1	3.2
	(TS-4) endo, ul	0.8	2.5	0.0	1.3
	(TS-5) exo, lk	4.2	2.8	2.7	3.1
	(TS-6) exo, ul	5.5	8.1	3.8	6.5
	(TS-7) endo, lk	5.4	5.0	3.8	2.9
	(TS-8) endo, ul	6.5	8.4	4.6	4.9

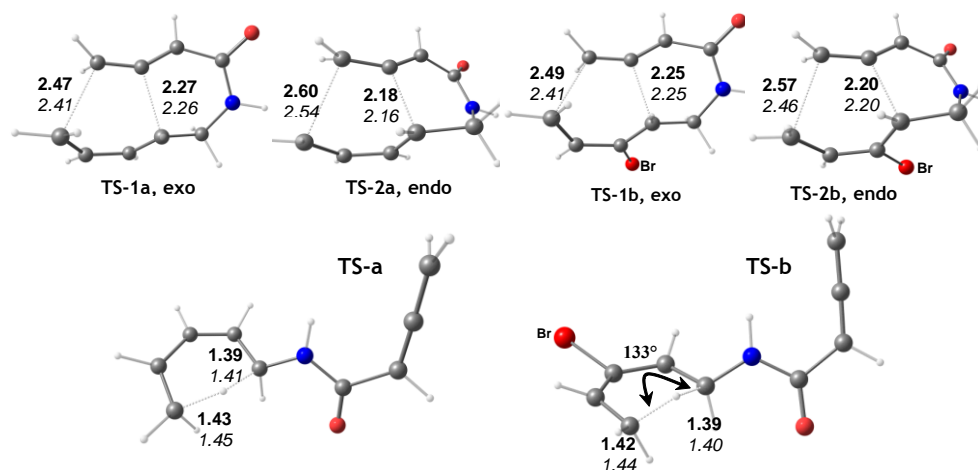
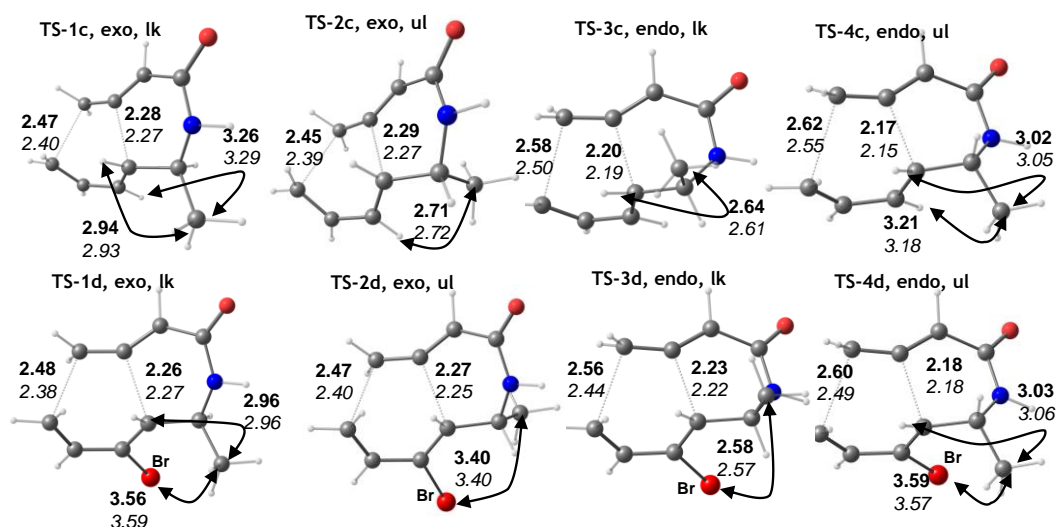
**Fig. 6.** Computed length (Å) of developing bonds for TS (Reactions **1a**, **1b**, **2a** and **2b**) at MP2/6-31G(d) (bold) and B3LYP/6-31G(d) (italics) level.**Fig. 7.** Computed geometries for TS (reactions **1c** and **1d**) at MP2/6-31G(d) (bold) and B3LYP/6-31G(d) (italics) level. Bond lengths are given in Å. Geometries for TS having a low product distribution are not presented.

Table 3. Computed bond lengths of the developing peripheral bond (r_1 , Å) and the developing internal bond (r_2 , Å) in TS* of IMDA Reactions **1a-d** (Fig. 2, Fig. 3).

TS	r_1 , Å		r_2 , Å		$\Delta r = r_1 - r_2$, Å	
	B3LYP/6-31G(d)	MP2/6-31G(d)	B3LYP/6-31G(d)	MP2/6-31G(d)	B3LYP/6-31G(d)	MP2/6-31G(d)
Intermolecular TS**	2.357		2.261		0.10	
TS-1a, exo	2.408	2.469	2.258	2.274	0.15	0.20
TS-2a, endo	2.540	2.602	2.158	2.179	0.38	0.42
TS-1b, exo	2.407	2.489	2.247	2.253	0.16	0.24
TS-2b, endo	2.464	2.573	2.203	2.198	0.26	0.38
TS-1c, exo, lk	2.397	2.471	2.269	2.278	0.13	0.19
TS-2c, exo, ul	2.386	2.453	2.268	2.285	0.12	0.16
TS-3c, endo, lk	2.499	2.580	2.187	2.202	0.31	0.38
TS-4c, endo, ul	2.546	2.616	2.152	2.174	0.39	0.44
TS-1d, exo, lk	2.381	2.479	2.269	2.264	0.11	0.22
TS-2d, exo, ul	2.400	2.468	2.252	2.269	0.15	0.20
TS-3d, endo, lk	2.439	2.545	2.218	2.226	0.22	0.32
TS-4d, endo, ul	2.489	2.597	2.178	2.183	0.31	0.41

* Bond lengths for the TS having a low product distribution are not presented; ** TS of Intermolecular Diels-Alder reaction of propadiene and 1,3-butadiene [8].

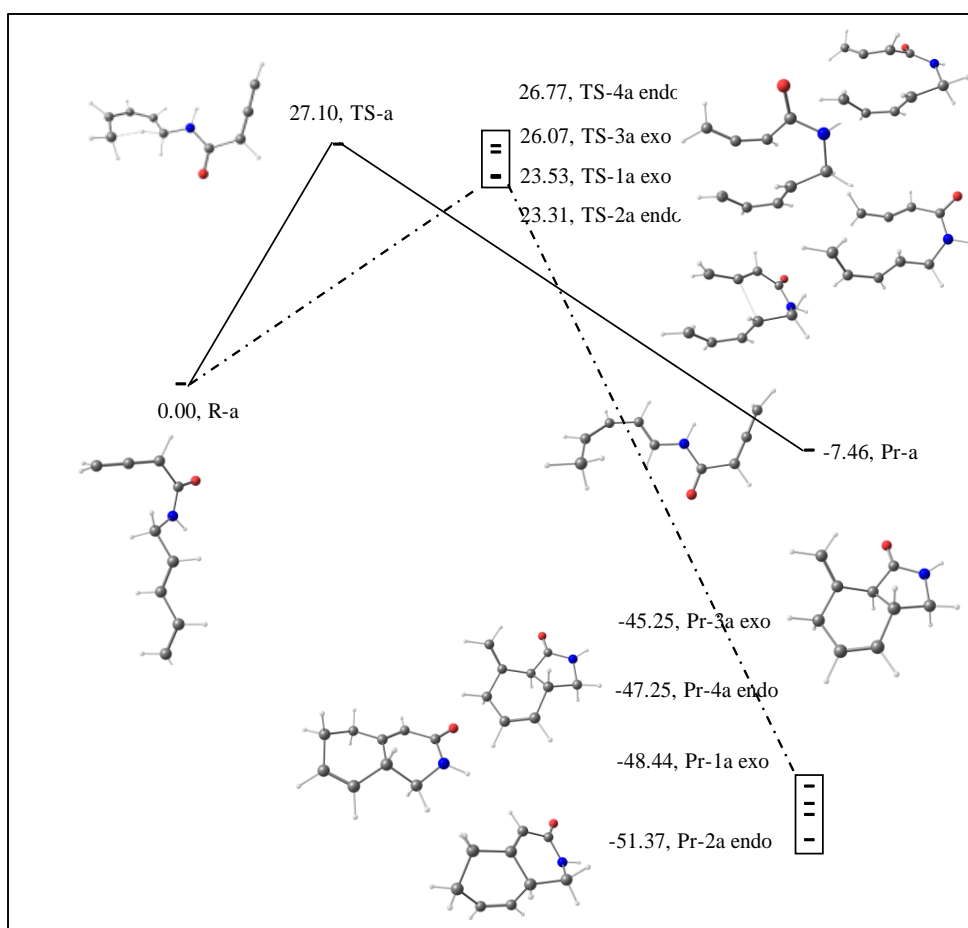


Fig. 8. Free energy profiles for reactions **1a** (—) and **2a** (---). The relative free energies (ΔG^\ddagger and ΔG) given in kcal.mol⁻¹ are computed at MP2/6-31G(d) level of theory (Table 1).

In contrast, DFT computations favored *reaction paths 2a, 2b* (Fig. 4) [1,5]-sigmatropic shift and subsequent Intramolecular [4+2] cycloaddition and hence the yielding of (**Z**) and (**E**) cycloadducts (Fig. 1, *reaction path 2*) with a more active in

IMDA reactions 1-methyl substituted diene moiety. The methyl SDG shifted reaction path toward Diels-Alder reaction and hence the group changed *regioselectivity*. The B3LYP/6-31G(d) exo cycloadducts - (**Pr-1a**), **exo** (*reaction 1a*) and (**Pr-**

1b), **exo** (reaction **1b**) - were preferred. Bromine SDG shifted the product ratio towards the trans-fused (**exo**) cycloadduct (Fig. 2). Use of SDG led to decreasing activation free energy of Diels-Alder reaction and accelerates the reaction rate (Table 1). Computed relative free energy differences of the favored products (**Pr-1c**) **exo**, **lk** and (**Pr-4c**), **endo**, **ul** by DFT and MP2 methods for reaction **1c** were opposite (Table 2).

Distances between C5 substituent and C3 connected H atom (causing destabilizing ^{1,3}A strain) and C5 substituent and C4 connected H atom (causing destabilizing eclipsing interactions) were optimized in the preferred products (**Pr-1c**) **exo**, **lk** and (**Pr-4c**), **endo**, **ul** (Fig. 7). When C3 and C5 substituents were incorporated in the precursor (**R-d**) a similar results were computed at MP2/6-31G(d) and B3LYP/6-31G(d) levels and reaction **1d** (Fig. 3) was found to be stereoselective.

Generally, the *steric effects* appear more important than the *electronic* ones in the IMDA reactions, especially in the presence of C3 and C5 substituents. C5 methyl substituent switches reaction paths **1** and **2** according to DFT calculations. Both methods are in agreement that in the presence of bromine and methyl substituents at C3 and C5 positions stereochemical outcome shifts toward (**exo**) cycloadduct.

Acknowledgements: This paper is supported by the Project BG051PO001-3.3.06-0003 "Building and steady development of PhD students, post-PhD and young scientists in the areas of the natural, technical and mathematical sciences". The Project is realized by the financial support of the Operative Program "Development of the human resources" of the European social fund of the European Union. The calculations were performed on Supermicro A+ Server 4042G-TRF, CPU AMD

Opteron 16 Cores Abu Dhabi 6376 2.30GHz, purchased with funds from the Project DFNI IO1/7, realized by financial support of Bulgarian National Science Fund.

REFERENCES

1. A. G. Fallis, *Can. J. Chem.*, **62**, 183 (1984).
2. D. Craig, *Chem. Soc. Rev.*, **16**, 187 (1987).
3. M. K. Diedrich, F-G. Klärner, B. R. Beno, K. N. Houk, H. Senderowitz, W. Clark Still, *J. Am. Chem. Soc.*, **119**, 10255 (1997).
4. D. J. Tantillo, K. N. Houk, M. E. Jung, *J. Org. Chem.*, **66**, 1938 (2001).
5. M. J. Lilly, M. N. Paddon-Row, M. S. Sherburn, C. I. Turner, *Chem. Commun.*, 2213 (2000).
6. T. Cayzer, L. Wong, P. Turner, M. N. Paddon-Row, M. S. Sherburn, *Chemistry*, 739 (2002).
7. R. Vijaya, G. N. Sastry, *J. Mol. Struct.: THEOCHEM*, **617**, 201 (2002).
8. M. Nendel, L. Tolbert, L. Herring, M. Islam, K. N. Houk, *J. Org. Chem.*, **64**, 976 (1999).
9. M. Manohan, P. Venuvanalingam, *J. Chem. Soc., Perkin Trans. 2*, 1423 (1996).
10. A. A. Granovsky, Firefly version 8.0.0, <http://classic.chem.msu.su/gran/firefly/index.html>
11. M. W. Schmidt, K. K. Baldrige, J. A. Boatz, S. T. Elbert, M. S. Gordon, J. J. Jensen, S. Koseki, N. Matsunaga, K. A. Nguyen, S. Su, T. L. Windus, M. Dupuis, J. A. Montgomery, *J. Comput. Chem.*, **14**, 1347 (1993).
12. V. Guner, K. S. Khuong, A. G. Leach, P. S. Lee, M. D. Bartberger, K. N. Houk, *J. Phys. Chem. A*, **107**, 11445 (2003).
13. V. A. Guner, K. S. Khuong, K. N. Houk, A. Chuma, P. Pulay, *J. Phys. Chem. A*, **108**, 2959 (2004).
14. D. H. Ess, K. N. Houk, *J. Phys. Chem. A*, **109**, 9542 (2005).
15. S. N. Pieniazek, F. R. Clemente, K. N. Houk, *Angew. Chem. Int. Ed. Engl.*, **47**, 7746 (2008).

ТЕОРЕТИЧНО ИЗСЛЕДВАНЕ НА СТЕРЕОСЕЛЕКТИВНОСТТА НА
ВЪТРЕШНОМОЛЕКУЛНА РЕАКЦИЯ НА ДИЛС-АЛДЕР НА 2,4-ПЕНТАДИЕНИЛ
БУТАДИЕНАМИДИ С УЧАСТИЕТО НА КОНТРОЛИРАЩИ
СТЕРЕОСЕЛЕКТИВНОСТТА ГРУПИ

А. Ж. Патлеева*, Д. Д. Енчев, Г. Д. Нейков

Факултет по природни науки, Шуменски университет „Епископ Константин Преславски“, Шумен, България

Постъпила на 29 април 2014 г.; Коригирана на 26 май 2014 г.

(Резюме)

Конкуриращи се вътрешномолекулни перициклични реакции на 2,4-пентадиенил бутадиенамиди (вътрешномолекулна реакция на Дилс-Алдер; [1,5]-сигматропна прегрупировка и следващо [4+2] циклоприсъединяване; Алдер-ене реакция) са моделирани като асинхронни съгласувани процеси с полуемпирични, *ab initio* и DFT теоретични методи. Изследвана е промяната в регио- и стереоселективността на вътрешномолекулните реакции с помощта на контролиращи съотношението между стереоизомерите заместители на C3 и C5 позиция. Предпочитаните циклоадукти са определени от относителните енергии на моделираните преходни структури.